

JPhys Energy

PAPER • OPEN ACCESS

Time-resolved *in-situ* x-ray diffraction study of CaO and CaO:Ca₃Al₂O₆ composite catalysts for biodiesel production

To cite this article: A Damiano Bonaccorso *et al* 2021 *J. Phys. Energy* **3** 034014

View the [article online](#) for updates and enhancements.



PAPER

OPEN ACCESS

RECEIVED
2 February 2021REVISED
10 May 2021ACCEPTED FOR PUBLICATION
21 May 2021PUBLISHED
28 June 2021

Original content from
this work may be used
under the terms of the
[Creative Commons
Attribution 4.0 licence](#).

Any further distribution
of this work must
maintain attribution to
the author(s) and the title
of the work, journal
citation and DOI.



Time-resolved *in-situ* x-ray diffraction study of CaO and CaO:Ca₃Al₂O₆ composite catalysts for biodiesel production

A Damiano Bonaccorso^{1,*}, Despoina Papargyriou¹, Aida Fuente Cuesta¹, Oxana V Magdysyuk², Stefan Michalik², Thomas Connolley², Julia L Payne^{1,*}  and John T S Irvine^{1,*} 

¹ School of Chemistry, University of St Andrews, North Haugh, KY16 9ST St Andrews, United Kingdom

² Diamond Light Source, Harwell Science and Innovation Campus, OX11 0DE Didcot, United Kingdom

* Authors to whom any correspondence should be addressed.

E-mail: jlp8@st-andrews.ac.uk, adb56@st-andrews.ac.uk and jtsi@st-andrews.ac.uk

Keywords: *in-situ*, operando, biodiesel, heterogeneous catalysis, waste to energy

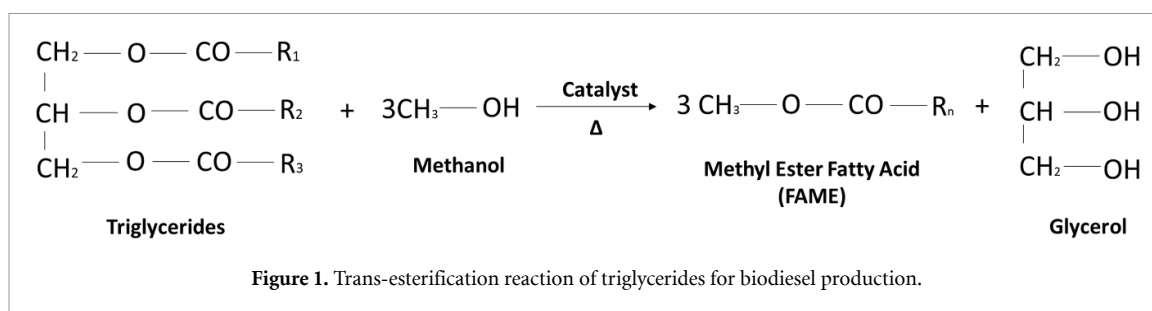
Supplementary material for this article is available [online](#)

Abstract

Alternative and sustainable waste sources are receiving increasing attention as they can be used to produce biofuels with a low carbon footprint. Waste fish oil is one such example and can be considered an abundant and sustainable waste source to produce biodiesel. Ultimately this could lead to fishing communities having their own ‘off-grid’ source of fuel for boats and vehicles. At the industrial level, biodiesel is currently produced by homogeneous catalysis because of the high catalyst activity and selectivity. In contrast, heterogeneous catalysis offers several advantages such as improved reusability, reduced waste and lower processing costs. Here we investigate the phase evolution of two heterogeneous catalysts, CaO and a Ca₃Al₂O₆:CaO (‘C3A:CaO’) composite, under *in-situ* conditions for biodiesel production from fish oil. A new reactor was designed to monitor the evolution of the crystalline catalyst during the reaction using synchrotron powder x-ray diffraction. The amount of calcium diglyceride (CaDG) began to increase rapidly after approximately 30 min, for both catalysts. This rapid increase in CaDG could be linked to *ex-situ* nuclear magnetic resonance studies which showed that the conversion of fish oil to biodiesel rapidly increased after 30 min. The key to the difference in activity of the two catalysts appears to be that the Ca₃Al₂O₆:CaO composite maintains a high rate of CaDG formation for longer than CaO, although the initial formation rates and reaction kinetics are similar. The Ca for the CaDG mainly comes from the CaO phase. In addition, towards the end of the second test utilising the CaO catalyst (after 120 min), there is a rapid decrease in CaDG and a rapid increase in Ca(OH)₂. This was not observed for the Ca₃Al₂O₆:CaO catalyst and this is due to Ca₃Al₂O₆ stabilising the CaO in the composite material. No additional calcium containing intermediate crystalline phases were observed during our *in-situ* experiment. Overall this specialised *in-situ* set-up has been shown to be suitable to monitor the phase evolution of heterogeneous crystalline catalysts during the triglycerides transesterification reaction, offering the opportunity to correlate the crystalline phases to activity, deactivation and stability.

1. Introduction

Due to the rapid development of modern industry and the service industry, serious problems caused by environmental pollution and the energy crisis are driving researchers to look for new energy sources [1]. Biodiesel is a tangible and sustainable alternative to conventional fossil fuels because it can be produced from naturally obtained renewable sources, such as plant oil, animal fat, and microorganisms. Oil from fish can be a promising and abundant source of sustainable feedstock for the production of biodiesel. Waste fish oil is categorised as a second generation biofuel, as the raw materials come from waste products rather than feedstocks traditionally used for food. As a result, the use of waste products results in more sustainable biodiesel. This is advantageous as it avoids the use of land that would normally be used for growing crops for



food [2]. In fact, due to the increase of aquaculture in the last decade, it is predicted that in 2030 the amount of fish consumed will increase by 30 million tonnes compared to 2016 [3]. This will be translated to an increase of the waste stream, which contains 25%–30% of waste oils [4]. The use of this waste fish oil will be cheaper and more sustainable than other biofuels, whilst also requiring less land [5]. As a result, the generation of biodiesel from waste products is particularly attractive to industry and communities in rural areas as it offers one way of readily providing power when isolated from the grid.

Biodiesel is generally produced by the transesterification reaction of vegetable oils or animal fats with an alcohol in the presence of an acidic catalyst (i.e. hydrochloric acid, sulphuric acid) or basic conditions (i.e. sodium hydroxide, sodium methoxide) (figure 1). The catalyst is required to initiate the reaction and behave as a solubiliser, as the alcohol is sparingly soluble in the oil phase, and non-catalysed reactions are particularly slow. The catalyst promotes an increase in alcohol solubility to allow the reaction to proceed at a reasonable rate [6]. Further improvements of the sustainability of biodiesel could be used through the use of ethanol produced by biomass fermentation rather than methanol [2].

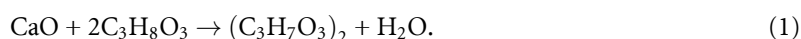
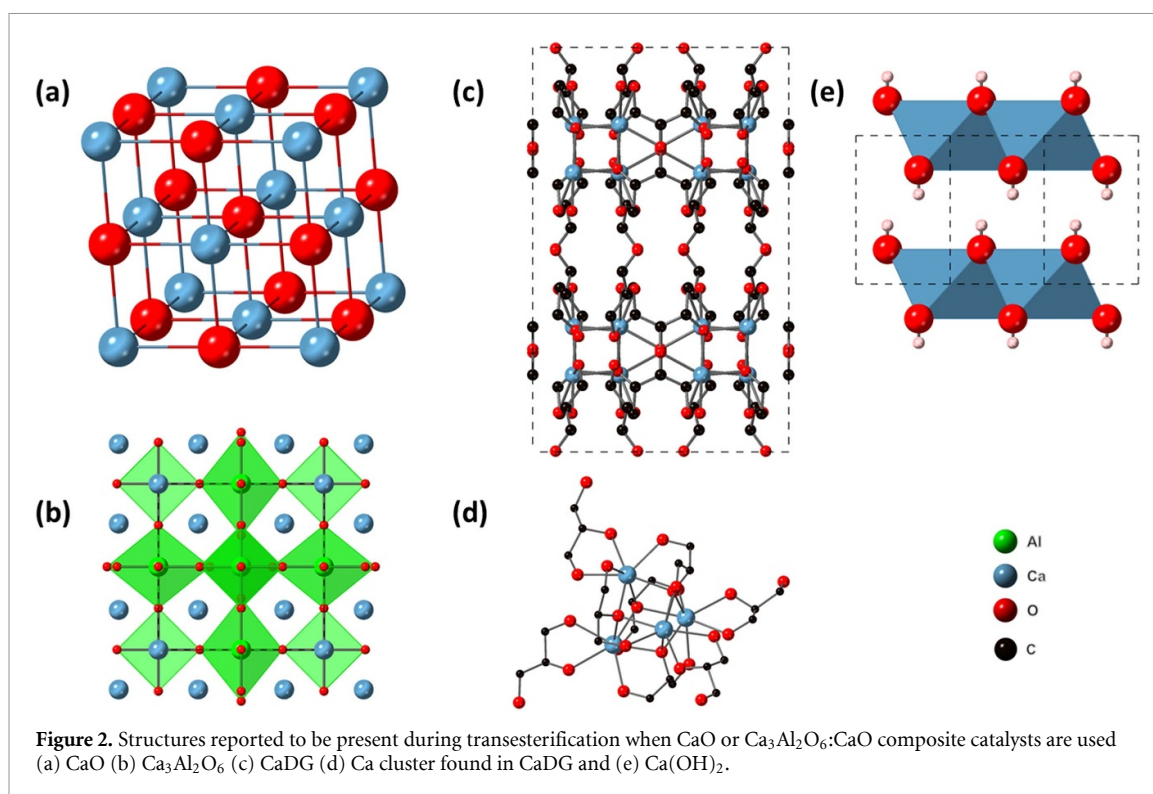
The production of biodiesel by homogeneous catalysis is a mature process widely used at the industrial level because these catalysts demonstrate fast reaction rates, low cost, and are easy to use. However, this technology has limitations because the homogenous catalyst contaminates the biodiesel. As a result extra separation and purification steps are required which increases the cost and energy requirements of biodiesel production [7–10]. In addition, after the reaction, the catalyst has to be neutralised or removed with a large amount of hot water, which generates a large amount of industrial wastewater [9]. This has led to the utilisation of heterogeneous catalysts for the production of biodiesel as they offer many benefits for biodiesel production. These catalysts can be easily separated from the reaction mixture and recycled, are less corrosive and can be used in a continuous reactor, leading to a safer, cheaper, and more environmentally friendly operation. In addition, fewer separation steps are required than when using homogeneous catalysts. Heterogeneous catalysts do not leave neutralisation salts in glycerol and can be separated from the main product directly in the reactor by filtration [10]. As a result, biodiesel production is more economically feasible and environmentally friendly [11–13].

A variety of solid base catalysts have been investigated for this purpose. In particular, scientists have studied alkaline earth oxides, such as CaO, MgO and SrO due to their strong basic sites, which are beneficial to the transesterification reaction and show high catalytic activity [8, 14]. Particular attention has been paid to calcium oxide, and calcium oxide-based materials because these catalysts are low-cost materials, with high basicity, low solubility in methanol and demonstrate high activities under moderate reaction conditions [15–17].

Many researchers have reported that the transesterification reaction catalysed by CaO exhibits an S-shaped kinetic curve [18–20]. The curve shows a low induction period derived mainly from the mass transfer limitations since a three-phase system is used for this transesterification. Xiaobing Chen suggests that this induction period is limited by the mass transfer in the three-phase system and the formation of calcium mono-glyceroxide and calcium diglyceroxide (CaDG) boost the reaction because they act as surfactants, improving the miscibility of the components reactant [19].

CaDG has also been investigated as a catalyst for biodiesel production showing good performance and stability compared to CaO, which leached calcium (Ca^{2+}) ions influencing the quality of the final product. Leached calcium ions react with the free fatty acid (FFA) of oil, which leads to saponification and deactivates the practical function of the catalyst. Further advantages of CaDG are the low solubility in methanol and high resistance to atmospheric agents such as H_2O and CO_2 . There is evidence that the use of suitable supporting materials reduces leaching of Ca^{2+} ions and this helps the development of a continuous flow reactor [16, 21–26].

In our previous study, we reported the performance of a novel $\text{Ca}_3\text{Al}_2\text{O}_6:\text{CaO}$ (C3A:CaO) composite material which has demonstrated excellent stability due to the interaction between the two phases and high reactivity due to the formation of CaDG according to the equation (1)



However, the stability test carried out on this catalyst showed that after seven cycles, it was wholly deactivated due to the formation of Ca(OH)₂ [26]. Although heterogeneous catalysts for biodiesel production have been widely investigated, the relationship between the structure of a catalyst and its activity and stability are not known in some critical cases. Hence, carrying out *in-situ* experiments are considered to be essential because the catalyst undergoes structural and compositional changes which cannot be monitored by *ex-situ* studies. *In-situ* and *operando* studies utilising powder x-ray diffraction (PXRD) are powerful techniques used to reveal the presence of different phases under a range of operating conditions and reaction conditions [27–29].

Figure 2 shows the different structures reported during the catalytic testing of CaO and C3A:CaO composite catalysts. CaO adopts the rock-salt structure, whilst Ca₃Al₂O₆ consists of a network of corner sharing AlO₆ and AlO₄ units, with Ca sitting in the centre of the cavities and also at the corners of the cube. The crystal structure of CaDG consists of four Ca²⁺ ions arranged in a tetrahedron (as shown in figure 2(d)). There are four of these Ca clusters in the unit cell. Each Ca centre is coordinated by seven oxygens from the glyceroxide molecules. There are two symmetry inequivalent glyceroxide molecules in the unit cell, with Ca being coordinated by five oxygen molecules from one type of glyceroxide and the remaining two oxygens coming from the second type of glyceroxide. In the second type of glyceroxide molecule, only two out of three oxygens on the glyceroxide are bound to the Ca, leaving one oxygen-free. Ca(OH)₂ is reportedly formed upon catalyst deactivation or when CaO is in contact with H₂O in the atmosphere. Ca(OH)₂ has a layered structure, consisting of edge-sharing octahedra with the H of the (OH) groups pointing in between the layers.

To understand the kinetic reaction and the deactivation mechanisms of the CaO and C3A:CaO composite catalysts, we performed *in-situ* experiments on the I12 beamline at Diamond Light Source. The optimum composition of the C3A:CaO catalyst (with a ratio of Ca to Al of 6:1) was based on the activity and stability determined in previous work [26]. The aim of the *in-situ* PXRD studies was to monitor the phase evolution of the Ca containing species (CaO/Ca₃Al₂O₆ (C3A) /Ca(OH)₂/CaDG) during the transesterification reaction of triglycerides and correlate it to the performance, stability and deactivation of the catalyst during the different cycles. We should point out that this work offers several advantages over our previous work [26]. Firstly, by carrying out a time resolved *in-situ* reaction, it will allow us to monitor when each phase forms during the reaction, rather than simply looking at the catalyst at the end of the reaction under *ex-situ* conditions, where post-reaction work-up (i.e. the catalyst washing and recovery process) could have changed the catalysts. Secondly, it also allows us to investigate the differences between the two best

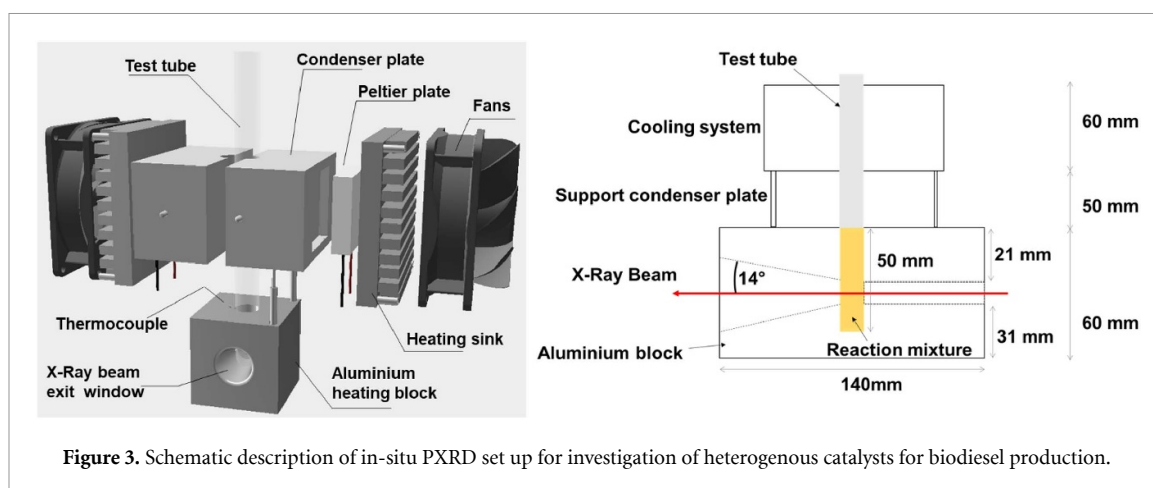


Figure 3. Schematic description of in-situ PXRD set up for investigation of heterogeneous catalysts for biodiesel production.

performing catalysts identified in our previous studies (CaO and C3A:CaO (Ca/Al 6:1)) when subjected to *in-situ* conditions. Thirdly, it allows us to understand whether the CaDG is the only species that catalyses the transesterification or whether there are new intermediate phases forming that favour the transesterification reaction. Furthermore the *in-situ* experiment also allows us to probe whether crystalline products such as CaDG, CaO and Ca(OH)₂ are formed with Ca from CaO or Ca₃Al₂O₆.

These tests were carried out using a novel *in-situ* XRD waterless reflux reactor operating in batch mode developed between Diamond Light Source and the University of St Andrews. The understanding of this reaction system helps to improve the current catalytic systems, e.g. by increasing reaction rates and catalyst stability. The synthesis of a highly active and stable heterogeneous catalyst for the production of biodiesel can offer several benefits for the commercialisation of this system, and also be applied in a continuous process, which can drastically reduce the capital cost of the current processes.

2. Experimental

2.1. Synthesis of the catalysts and characterisation of CaO-C3A composite material

The catalysts were prepared by combustion synthesis with ethylene glycol and citric acid, as reported previously [26]. A composite catalyst, consisting of CaO and Ca₃Al₂O₆ (C3A) with Ca/Al ratios equal to 6, was investigated. This was identified as the optimum composition, according to our previous study [26]. Commercial CaO powder from Sigma Aldrich 98% was calcined at 900 °C and was used as a reference. The conversion of fish oil to biodiesel at the end of the *in-situ* experiment was measured using proton nuclear magnetic resonance (¹H NMR) spectroscopy to ensure the completion of the reaction, as reported in our previous work [26]. The reaction went to completion in all cases.

The evaluation of the catalysts' activity for the trans-esterification reaction was performed with commercial cod liver oil, purchased from Holland and Barrett, UK. The FFA composition of the fish oil was reported in our previous study [26]. It consists mainly of palmitic acid (14.2%), oleic acid (13.8%), palmitoleic acid (11.7%), docosahexaenoic acid (11.2%), eicosapentaenoic acid (9.6%) and *cis*-11-eicosenoic acid (9.1%) [26].

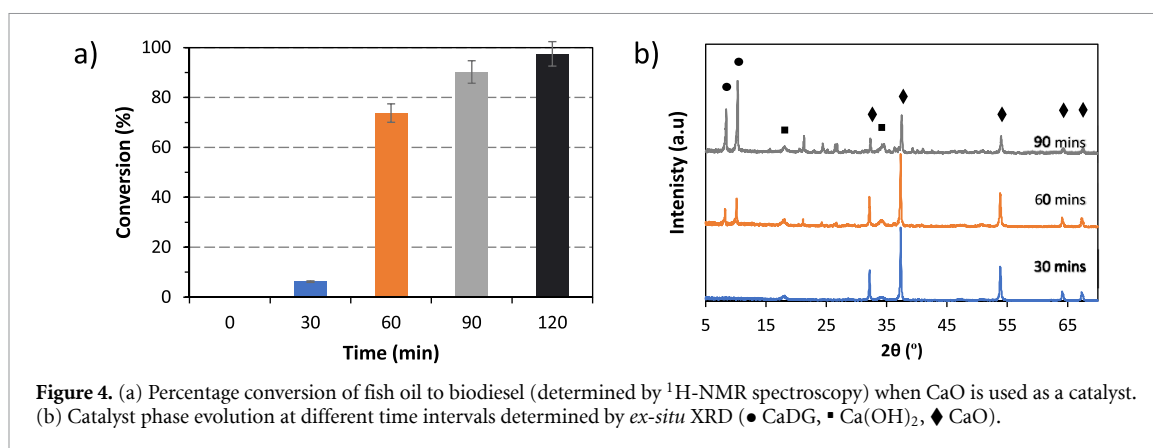
2.2. In-situ PXRD set-up

A novel *in-situ* set-up for PXRD analysis of heterogeneous catalysts for biodiesel production was developed for the experiment (figure 3). The set-up was composed of several parts: an aluminium heating block and two aluminium condenser plates, two CPU fans and two Peltier plates in the cooling system. A borosilicate tube (OD: 18 mm, ID: 14 mm, L: 200 mm) was used as a reaction chamber.

The aluminium block was designed to host and heat the borosilicate tube. The block was drilled in such a way that permitted the beam to pass through the borosilicate tube (see figure 3). The x-ray beam exit window was designed in a conical shape with an angle of 14° to allow the unobstructed exit of the diffracted x-rays.

The aluminium block was heated using a hotplate stirrer. The temperature of the reaction mixture was maintained at 65 °C over the course of the reaction and a thermocouple was used to monitor the temperature. The magnetic stirrer motor of the hotplate was used to mix the reactants and catalysts inside the borosilicate tube using a cross-shaped magnetic stirrer bar.

Key to the reactor design is the water-free reflux system. This was achieved by the use of a cooling system, made from condenser plates, fans, and Peltier plates (figure 3). The cooling system was switched-on before heating the solution to ensure the reflux of methanol during the reaction. The temperature of the Peltier



cooling plate (Aussel TEC1-12705 dimension 16 cm^2 12 V–45 W) was controlled by a PWM DC adjustable speed step-less 3–12 V drive board. A 5 V power supply controlled the CPU fans which provided airflow to cool the heat sink sitting on the Peltier cooling plate. The condenser plates were designed to have perfect contact with the borosilicate test tube and guaranteed a large surface area (67.85 cm^2), enabling reflux conditions to be maintained during the reaction.

2.3. PXRD *in-situ* studies

In-situ synchrotron PXRD experiments were performed on the I12 (Joint Engineering, Environmental and Processing ‘JEEP’) beamline at Diamond Light Source [30]. The wavelength of the incident x-ray beam and diffraction geometry were determined by measuring a NIST Standard Reference Material 674b CeO_2 sample at different standard-to-detector distances following Hart *et al* approach [31]. The wavelength of the incident beam was 0.23112 \AA . The x-ray beam size was $0.5 \times 0.5\text{ mm}$. Data were collected in transmission mode using a Pilatus 2M CdTe area detector. The exposure time for a single diffraction pattern was 20 s. Diffraction data were continuously collected over a period of 3 h to monitor the transesterification reaction.

The collected two-dimensional diffraction data were azimuthally integrated into one-dimensional intensity curves using the DAWN software [32, 33].

Sequential multiphase Rietveld refinement was carried out using Topas Academic v6 [34].

The transesterification reaction was performed in a borosilicate test tube (ID: 18 mm OD:15 mm L: 180 mm). The oil, methanol and catalyst were mixed in a ratio 1:12:10, and the resultant solution was stirred in the test tube by using a magnetic stirrer (1100–1200 rpm). The reaction was carried out at $65\text{ }^\circ\text{C}$ for a period of 3 h following the experimental parameters optimised in our previous work [26]. At the end of the first 3 h period (i.e. the ‘first test’), the whole reaction mixture was centrifuged at 1400 rpm, the liquid was decanted, and the remaining catalyst was filtered under vacuum and washed thoroughly with methanol. Then, the recovered catalyst was dried in the oven ($80\text{ }^\circ\text{C}$) overnight, and it was used for a second test. The conversion of the fish oil triglycerides to the methyl esters of the biodiesel was determined at the end of the reaction by $^1\text{H NMR}$ spectroscopy using a Bruker AVII 400 spectrometer [26, 35].

3. Results and discussions

Our previous work reported the morphology and particle size of the CaO and C3A:CaO catalysts prepared using the same method as used in this paper and showed that the particle size of CaO are smaller and less agglomerated than C3A [26]. Prior to carrying out the *in-situ* XRD study, catalytic testing was performed in the lab-scale reactor with CaO as catalyst, according to the method described previously by Papargyriou *et al* [26]. The percentage conversion of fish oil to biodiesel was determined using $^1\text{H-NMR}$ spectroscopy. Figure 4(a) shows a large increase in the conversion of fish oil to biodiesel (from 7% to 75%) between 30 and 60 min of catalytic testing. *Ex-situ* XRD of the recovered catalyst, performed at different time intervals, revealed that this increase in performance was accompanied by the gradual transformation of CaO to CaDG. This confirmed that the reactor that was designed for the *in-situ* XRD experiments, was suitable for biodiesel formation. This will allow us to monitor the phase evolution during the transesterification reaction and compare CaO and C3A:CaO catalysts, which have previously been shown to have different stabilities and probe intermediate crystalline species which could catalyse the transesterification reaction at the beginning of the reaction.

Figure S1 (available online at stacks.iop.org/JPENERGY/3/034014/mmedia) shows a typical diffraction pattern obtained during the *in-situ* experiment. The broad hump is due to the borosilicate test tube used to

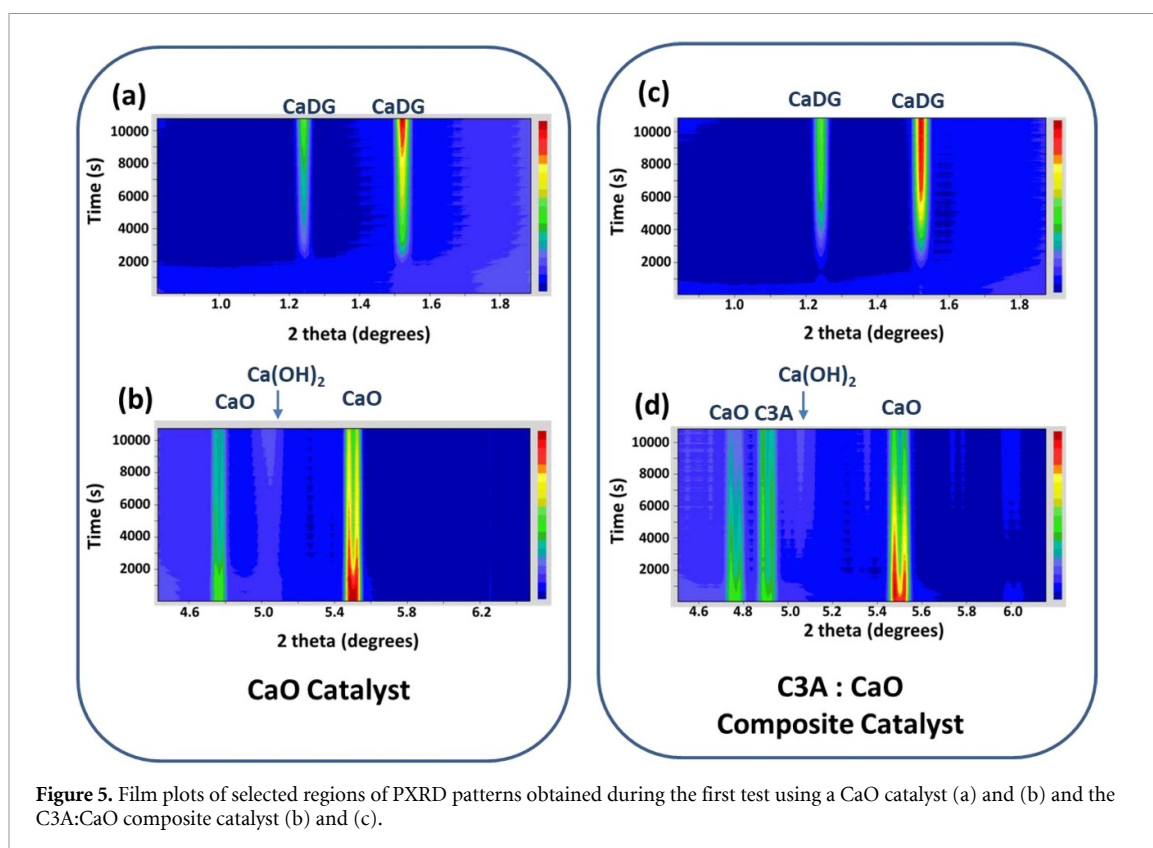


Figure 5. Film plots of selected regions of PXRD patterns obtained during the first test using a CaO catalyst (a) and (b) and the C3A:CaO composite catalyst (b) and (c).

contain the reaction mixture, as well as the non-crystalline fish oil and biodiesel. Peak splitting is clearly observed, due to stirring of the reaction mixture. Multiphase sequential Rietveld refinement was carried out in order to extract phases fractions (expressed as weight per cent) from the data. Prior to the sequential refinements, peak profile parameters for each phase were obtained by fitting the first and last data sets. The resulting peak profile parameters were fixed during the refinement. A Chebyshev polynomial with 30 terms was used to model the background. The scale factor and lattice parameters were allowed to refine for each phase. In the cases where peak splitting was observed, one smaller and one large lattice parameter was used, in order to fit the data. The Rietveld fits at the beginning and end of testing for both the CaO and C3A:CaO composite catalysts are shown in figures S2 and S3. Unit cell parameters are given in table S1 and showed no significant changes over the course of the experiment.

Figure 5 shows the film plots of regions of the XRD patterns collected during the first test of CaO and C3A:CaO catalysts for biodiesel production, with increasing time. Initially, the main phase identified was CaO, or the $\text{Ca}_3\text{Al}_2\text{O}_6$ -CaO mixture expected for the C3A:CaO catalyst. During the progression of the transesterification reaction and after approximately 30 min CaDG peaks observed in the diffraction patterns of both catalysts began to increase in intensity. This correlates with the increase in percentage biodiesel conversion (figure 4(a)) which is observed after 30 min. CaDG forms when CaO reacts with the glycerol by-product of the transesterification reaction (equation (1)). As reported by Esipovich *et al* the diglycerol oxide species are formed in two different steps. Firstly, the calcium oxide reacts with methanol to form CH_3O^- and OH^- groups on the CaO surface, and then these groups are replaced by glycerol leading to formation of the more stable CaDG [33]. As the reaction proceeded, the formation of the CaDG phase continued and the intensities of the corresponding CaDG peaks increased gradually for both catalysts, until the end of test 1 (180 min). Furthermore, the formation of $\text{Ca}(\text{OH})_2$ was observed to a small extent in both cases, which can be attributed to the hydration of CaO, due to presence of water in the reaction mixture. We should point out that the film plot in figures 5(a) and (c) shows the formation of CaDG both for the CaO and for the C3A:CaO catalysts. This shows that the C3A:CaO catalyst has a similar activation mechanism to CaO [20].

Figure 6 shows the evolution of the weight per cent of the crystalline components of the reaction mixture with time during the transesterification reaction for both catalysts. The duration of each test was fixed at 180 min (3 h), according to the optimisation of the system performed *ex-situ* in previous studies [26]. At the beginning of the first test for CaO (figure 6(a)), a small amount of $\text{Ca}(\text{OH})_2$ was observed in the diffraction patterns (approximately 11 wt%). After approximately 30 min, the amount of CaDG increased gradually,

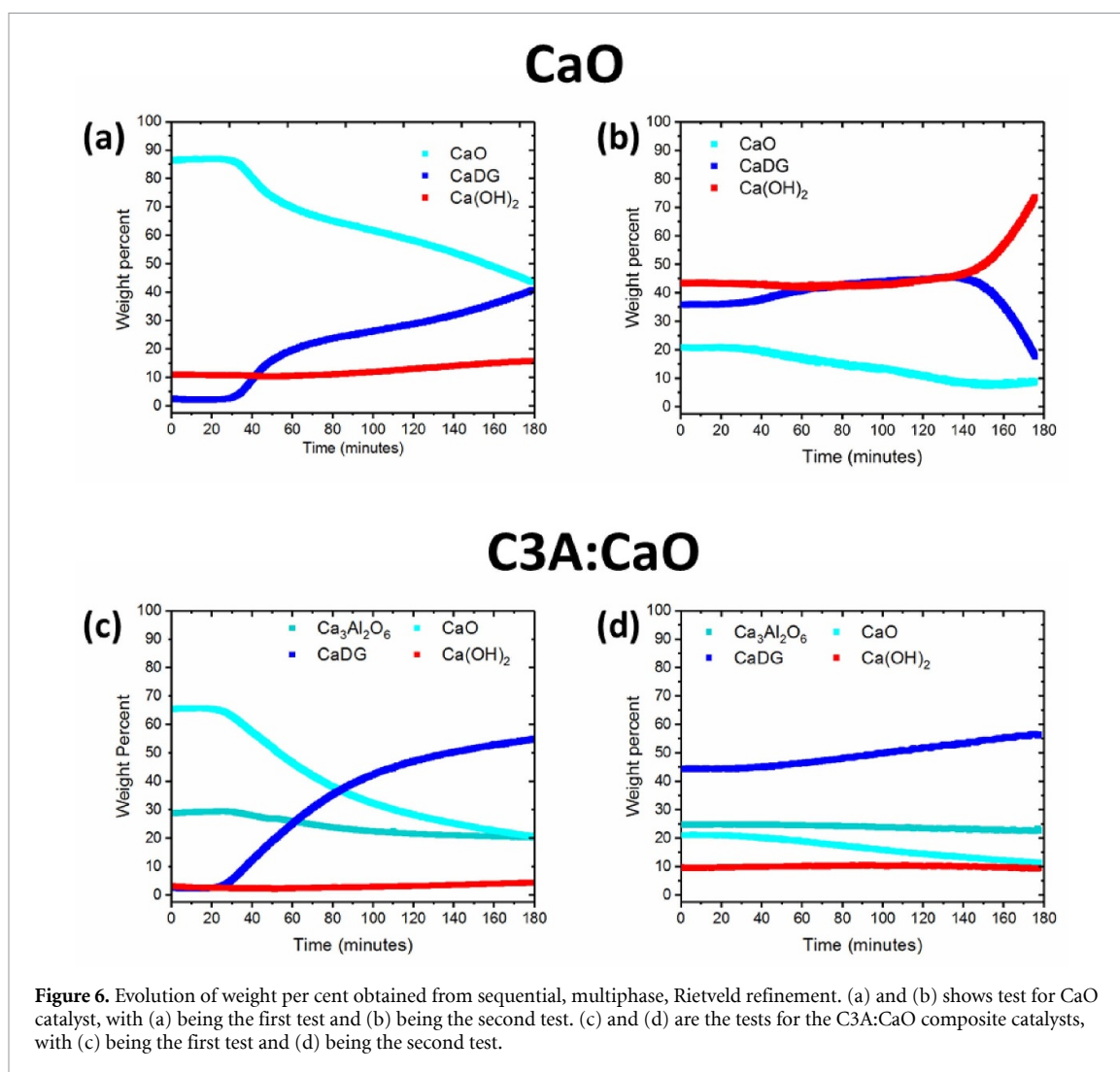


Figure 6. Evolution of weight per cent obtained from sequential, multiphase, Rietveld refinement. (a) and (b) shows test for CaO catalyst, with (a) being the first test and (b) being the second test. (c) and (d) are the tests for the C3A:CaO composite catalysts, with (c) being the first test and (d) being the second test.

while the CaO percentage decreased. The appearance of CaDG in the diffraction patterns can be correlated with the percentage conversion of fish oil to biodiesel (figure 4(a)). From 30 min (the point at which CaDG appears in the diffraction pattern), the biodiesel conversion increases rapidly, until 60 min, after which point the increase in percentage conversion is much slower. At the end of test 1 the relative weight per cent of the CaO phase decreased to 45%, CaDG increased to 40% and $\text{Ca}(\text{OH})_2$ slightly increased to 15%.

The formation of CaDG after 30 min indicates that initially, the transesterification reaction (figure 1) does not utilise CaDG. It seems that the presence both of CaO and $\text{Ca}(\text{OH})_2$ at the beginning of the test (figure 5) catalyses the transesterification reaction in the first 30 min to form enough glycerol to promote the formation of CaDG. For CaO, the catalytic action is generated by basic sites on the surface of CaO particles which creates nucleophilic alkoxides from alcohol, thus initiating the base-catalysed reaction. The methanolysis forms calcium methoxide $\text{Ca}(\text{OCH}_3)_2$ on the surface of CaO by the action of methanol. This theory was confirmed by Arzamendi *et al* and Xiangbing Chen *et al* and Oueda *et al* [14, 19, 36, 37]. The reaction is accelerated when the correct amount of glycerol is formed in the transesterification reaction and is able to react with CaO to form CaDG. This reaction showed an acceleration in the formation rate between 30 and 60 min and then continued at a slower rate (figures 6(a) and 4(a)). The acceleration is directly proportional to the formation rate of CaDG. The formation rate of CaDG shows an S-shaped curve which is in agreement with the shape of the conversion rate of the transesterification reaction of fatty acid methyl ester (FAME) as reported by Chen and our previous study [19, 26].

Figure 6(b) shows the evolution of the phases of the recycled CaO in the second catalytic test. The initial catalyst composition has changed during the catalyst recovery process (particularly the CaO:Ca(OH)₂ ratio, although the CaDG content of the catalyst remained approximately the same). The recovered catalyst mixture showed that the weight per cent of $\text{Ca}(\text{OH})_2$ increased while the weight per cent of CaO decreased. This variation implies that the CaO is transformed into $\text{Ca}(\text{OH})_2$ due to the hydration of the sample during the recycling process as widely reported in the literature [20, 38, 39].

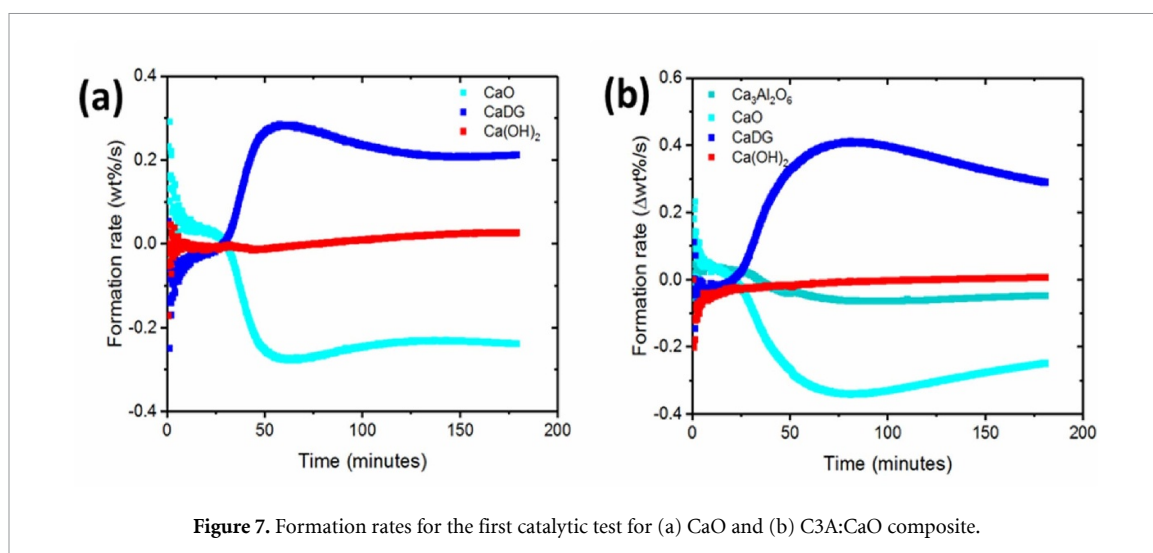


Figure 7. Formation rates for the first catalytic test for (a) CaO and (b) C3A:CaO composite.

The CaO lost between test 1 and test 2 can be attributed to CaO leaching into biodiesel and glycerol oxide and difficulty in recovering the catalyst for the second test, as reported by Furusawua *et al* [40]. On the other hand, the amount of CaDG did not change significantly, which shows that this phase is more stable during catalyst handling and which is probably due to its low solubility in the reaction mixture and low reactivity with environmental moisture. In the second test utilising CaO, after approximately 120 min, the amount of CaDG drastically decreased, while the Ca(OH)₂ phase increased significantly. According to the literature, in the presence of water, CaDG can be hydrolysed according to equation (2) [41]. An increased Ca(OH)₂ content in the catalyst is known to lead to the deactivation of the catalyst [26]

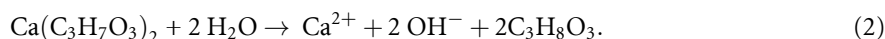


Figure 6(c) shows the first test for the C3A–CaO composite. The initial catalyst composition was 65 wt% CaO, 29 wt% C3A, 3 wt% of Ca(OH)₂ and 3 wt% of CaDG. The C3A:CaO composite catalyst follows the similar three step trend shown for CaO. In a similar fashion to CaO, after 30 min, CaDG increased dramatically. Again an increase of CaDG and a decrease of CaO was observed. The presence of C3A does not contribute to the catalytic performance as reported in the kinetic curve in our previous work, but the C3A phase acts as a stabiliser, anchors the active phase and consequently helps to increase the catalyst stability [25]. At the end of test 1, the CaO phase decreased to 21%, CaDG increased to 55%, C3A decreased to 20% and Ca(OH)₂ slightly increased to 4%.

Finally, figure 6(d) shows the evolution of the phases for the second test using C3A:CaO. This catalyst demonstrated better stability compared to pure CaO. Unlike the second test utilising CaO (figure 6(c)), no rapid decrease in weight per cent of CaDG or rapid increase in Ca(OH)₂ was observed at the end of the reaction. This indicates that the composite catalyst is more stable than the pure CaO catalyst. The C3A content remains constant throughout the second test (figure 6(c)). The reaction for the CaDG formation continued at a slower rate and no decrease was observed. This suggests that this catalyst shows superior stability compared to CaO and acts as a stabiliser for the active phase, while it does not participate in the reaction. Due to the enhanced stability of the composite catalyst, we were unable to confirm the crystalline phases responsible for the deactivation of this catalyst from this *in-situ* experiment.

In order to look at the difference in the formation rate of CaDG between the two catalysts, formation rates were calculated using the difference in weight per cent between time x and time = 0. A comparison of the formation rates for each catalyst is shown in figures 7(a) and (b). As can be seen in figure 7, the increase in CaDG formation rate occurs when there is a decrease in CaO formation (i.e. CaO gets used up). When the C3A:CaO composite catalyst is used, there is a higher decrease in CaO than in Ca₃Al₂O₆, indicating that the Ca in CaDG is mainly coming from the CaDG. When CaO is used as a catalyst, the Ca(OH)₂ content begins to increase towards the end of the catalyst test. However, when Ca₃Al₂O₆:CaO is used, the Ca(OH)₂ maintains a constant value of approximately 0 wt% s⁻¹, indicating that there is no substantial change during the reaction. This implies that the composite catalyst is more resistant to hydration or catalyst poisoning from ambient conditions.

The resulting comparison in the formation rates of CaDG for the CaO and C3A:CaO catalysts is shown in figure 8. As can be seen, the formation rate of CaDG increases sharply after 30 min for both catalysts, although the increase begins slightly sooner for the Ca₃Al₂O₆:CaO composite. Between $t = 25$ and

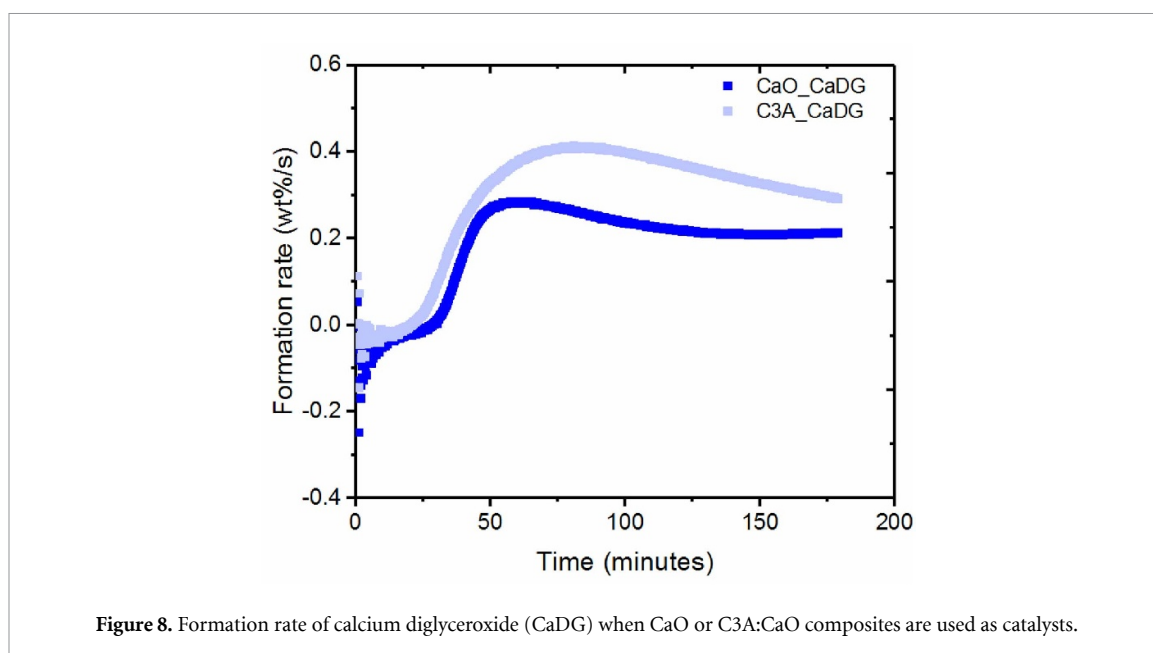


Figure 8. Formation rate of calcium diglyceride (CaDG) when CaO or C3A:CaO composites are used as catalysts.

$t = 50$ min, the gradient of the two curves is similar, indicating similar increases in the formation rates for both catalysts. However, when the C3A composite is used the formation rate of CaDG continues to increase beyond $t = 50$ min, up to approximately $t = 80$ min.

The different CaDG formation rate for the C3A:CaO composite suggests that alumina plays an important role in the performance of the CaO. Umdu *et al* reported that alumina increases the basicity and the basicity strength when CaO is supported on alumina [42]. The different formation rate could also be affected by the increase in active sites of the catalyst due to the CaO distribution in the $\text{Ca}_3\text{Al}_2\text{O}_6$ matrix of the composite catalyst.

4. Conclusions

We have successfully implemented and used a water-free reflux system, suitable for carrying out *in-situ* PXRD studies on heterogeneous catalysts. *In-situ* PXRD is an exciting technique to investigate the phase evolution of heterogeneous catalysts and this may be correlated with other data (e.g. $^1\text{H-NMR}$ spectroscopy) in order to begin to build up an understanding of activation and deactivation mechanisms. We studied the CaO and C3A:CaO catalysts as heterogeneous catalysts for biodiesel production from fish oil. The *in-situ* experiment allowed us to probe when different crystalline phases form, whether intermediate phases form, where the Ca comes from and finally the differences between the CaO and C3A:CaO composite catalysts. Multiphase Rietveld refinement shows that there is a significant decrease in CaO weight per cent as CaDG is produced, indicating that the Ca in CaDG mainly comes from CaO. No additional intermediate crystalline phases were observed in the PXRD data. Time-resolved PXRD studies of both catalysts are in agreement with previous work, which shows that the activation mechanism consists of two steps [16, 19–27]. The first step is catalysed by the basic oxygen of CaO and CaOH. It has a low reaction rate in the induction period and derives mainly from the mass transfer since a three-phase system is used for this transesterification [19]. The second activation step begins after around 30 min and is caused by the formation and rapid increase in the formation rate of CaDG for both catalysts. The formation of CaDG boosts the reaction rate of the transesterification reaction. This correlates with our *ex-situ* NMR studies which showed a large increase in biodiesel formation after 30 min (figure 4) [26]. The formation rate of CaDG is directly proportional to the oil conversion into FAME, and both show a typical S-shaped kinetic curve. Moreover, it was observed that the composite C3A:CaO demonstrated better stability compared to pure CaO. In the second test utilising CaO, after 120 min, there was a rapid decrease in the weight per cent of CaDG, accompanied by a rapid increase in $\text{Ca}(\text{OH})_2$, which is expected to result in catalyst deactivation. However, in the second test utilising the C3A:CaO catalyst, no rapid increase in $\text{Ca}(\text{OH})_2$ was observed, which indicates that this catalyst is more stable under reaction conditions than the CaO catalyst. The presence of $\text{Ca}_3\text{Al}_2\text{O}_6$ in the C3A:CaO catalyst had a dual effect on the catalyst: (a) to increase the stability of the CaO (b) to increase the conversion rate due to the high formation rate of the CaDG phase [25].

Finally, we expect that this set-up will be suitable for the study of other heterogeneous catalysts in the future. It will also be a useful tool to probe the phase evolution in heterogeneous catalysts in greater detail than would be possible using *ex-situ* studies alone.

Data availability statement

The data that support the findings of this study are openly available at the following URL/DOI: <https://doi.org/10.17630/313c6d61-f04d-4deb-9974-1d2dda459c12> [35].

Acknowledgments

The authors would like to acknowledge Innovate UK (Project Nos. 103498 and 106037) and EPSRC (EP/K015540/1 and EP/P007821/1) for funding. This work was carried out with the support of the Diamond Light Source, instrument I12 (proposal EE20820).

ORCID iDs

Julia L Payne  <https://orcid.org/0000-0003-3324-6018>

John T S Irvine  <https://orcid.org/0000-0002-8394-3359>

References

- [1] OECD 2011 Green Growth Studies (available at: www.oecd.org/greengrowth/greening-energy/49157219.pdf)
- [2] Ramos M, Dias A P S, Puna J F, Gomes J and Bordado J C 2019 *Energies* **12** 4408
- [3] FAO 2018 The State of World Fisheries and Aquaculture 2018—Meeting the sustainable development goals Rome (available at: <http://fao.org/3/i9540en/I9540EN.pdf>)
- [4] Girish C R, Gambhir M M and Desmukh H 2017 *Int. J. Civ. Eng. Technol.* **8** 01–06
- [5] Gnanaprakasam A, Sivakumar V M, Surendhar A, Thirumarimurugan M and Kannadasan T 2013 Recent strategy of biodiesel production from waste cooking oil and process influencing parameters: a review *J. Energy* **2013** 1–10
- [6] Xue W, Zhou Y-C, Song B-A, Shi X, Wang J, Yin S-T, Hu D-Y, Jin L-H and Yang S 2009 Synthesis of biodiesel from *Jatropha curcas* L. seed oil using artificial zeolites loaded with CH₃COOK as a heterogeneous catalyst *Nat. Sci.* **1** 55–62
- [7] Atabani E, Silitonga A S, Badruddin I A, Mahlia T M I, Masjuki H H and Mekhilef S 2012 A comprehensive review on biodiesel as an alternative energy resource and its characteristics *Renew. Sustain. Energy Rev.* **16** 2070–93
- [8] Lee A F, Bennett J A, Manayil J C and Wilson K 2014 Heterogeneous catalysis for sustainable biodiesel production via esterification and transesterification *Chem. Soc. Rev.* **43** 7887–916
- [9] Knothe G and Razon L F 2017 Biodiesel fuels *Prog. Energy Combust. Sci.* **58** 36–59
- [10] Knothe G 2010 Biodiesel and renewable diesel: a comparison *Prog. Energy Combust. Sci.* **36** 364–73
- [11] Diamantopoulos N, Panagiotaras D and Nikolopoulos D 2015 Comprehensive review on the biodiesel production using solid acid heterogeneous catalysts *J. Thermodyn. Catal.* **6** 1–8
- [12] Atadashi I M, Aroua M K, Abdul Aziz A R and Sulaiman N M N 2013 The effects of catalysts in biodiesel production: a review *J. Ind. Eng. Chem.* **19** 14–26
- [13] Chouhan A P S and Sarma A K 2011 Modern heterogeneous catalysts for biodiesel production: a comprehensive review *Renew. Sustain. Energy Rev.* **15** 4378–99
- [14] Oueda N, Bonzi-Coulibaly Y L and Ouédraogo I W K 2017 Deactivation processes, regeneration conditions and reusability performance of CaO or MgO based catalysts used for biodiesel production—a review *Mater. Sci. Appl.* **08** 94–122
- [15] Marinković D M, Stanković M V, Veličković A V, Avramović J M, Miladinović M R, Stamenković O O, Veljković V B and Jovanović D M 2016 Calcium oxide as a promising heterogeneous catalyst for biodiesel production: current state and perspectives *Renew. Sustain. Energy Rev.* **56** 1387–408
- [16] Kouzu M, Kasuno T, Tajika M, Sugimoto Y, Yamanaka S and Hidaka J 2008 Calcium oxide as a solid base catalyst for transesterification of soybean oil and its application to biodiesel production *Fuel* **87** 2798–806
- [17] Kesic Z, Lukic I, Zdujic M, Mojovic L and Skala D 2016 Calcium oxide based catalysts for biodiesel production: a review *Chem. Ind. Chem. Eng. Q.* **22** 391–408
- [18] Granados M L, Zafra Poves M D, Alonso D M, Mariscal R, Galisteo F C, Moreno-Tost R, Santamaría J and Fierro J L G 2007 Biodiesel from sunflower oil by using activated calcium oxide *Appl. Catal. B* **73** 317–26
- [19] Chen X, Li Z, Chun Y, Yang F, Haocheng X and Wu X 2020 Effect of the formation of diglycerides/monoglycerides on the kinetic curve in oil transesterification with methanol catalysed by calcium oxide *ACS Omega* **5** 4646–56
- [20] Esipovich A, Danov S, Belousov A and Rogozhin A 2014 Improving methods of CaO transesterification activity *J. Mol. Catal. A: Chem.* **395** 225–33
- [21] Kouzu M, Kasuno T, Tajika M, Yamanaka S and Hidaka J 2008 Active phase of calcium oxide used as solid base catalyst for transesterification of soybean oil with refluxing methanol *Appl. Catal. A* **334** 357–65
- [22] Hattori H, Shima M and Kabashima H 2000 Alcoholysis of ester and epoxide catalysed by solid base *Stud. Surf. Sci. Catal.* **130** 3507–12
- [23] Granados M L, Alonso D M, Sádaba I, Mariscal R and Ocón P 2009 Leaching and homogeneous contribution in liquid phase reaction catalysed by solids: the case of triglycerides methanolysis using CaO *Appl. Catal. B* **89** 265–72
- [24] Kouzu M, Yamanaka S-Y, Hidaka J-S and Tsunomori M 2009 Heterogeneous catalysis of calcium oxide used for transesterification of soybean oil with refluxing methanol *Appl. Catal. A* **355** 94–9
- [25] Taufiq-Yap Y H, Lee H V, Yunus R and Juan J C 2011 Transesterification of non-edible *Jatropha curcas* oil to biodiesel using binary Ca–Mg mixed oxide catalyst: effect of stoichiometric composition *Chem. Eng. J.* **178** 342–7

- [26] Papargyriou D, Broumidis E, de Vere-tucker M, Gavrielides S, Hilditch P, Irvine J T S and Bonaccorso A D 2019 Investigation of solid base catalysts for biodiesel production from fish oil *Renew. Energy* **139** 661–9
- [27] Breeze M I, Chamberlain T W, Clarkson G J, de Camargo R P, Wu Y, de Lima J F, Millange F, Serra O A, O'Hare D and Walton R I 2017 Structural variety in ytterbium dicarboxylate frameworks and *in situ* study diffraction of their solvothermal crystallisation *CrystEngComm* **19** 2424
- [28] Moorhouse S J, Wu Y, Buckley H C and O'Hare D 2016 Time-resolved *in situ* powder x-ray diffraction reveals the mechanisms of molten salt synthesis *Chem. Commun.* **52** 13865
- [29] Wu Y, Breeze M I, O'Hare D and Walton R I 2017 High energy x-rays for following metal-organic framework formation: identifying intermediates in interpenetrated MOF-5 crystallisation *Microporous Mesoporous Mater.* **254** 178–83
- [30] Drakopoulos M *et al* 2015 I12: the joint engineering, environment and processing (JEEP) beamline at diamond light source *J. Synchrotron Radiat.* **22** 828–38
- [31] Hart M L, Drakopoulos M, Reinhard C and Connolley T 2013 Complete elliptical ring geometry provides energy and instrument calibration for synchrotron-based two-dimensional x-ray diffraction *J. Appl. Cryst.* **46** 1249–60
- [32] Basham M *et al* 2015 Data analysis workbench (DAWN) *J. Synchrotron Radiat.* **22** 853–8
- [33] Filik J *et al* 2017 Processing two-dimensional x-ray diffraction and small-angle scattering data in DAWN 2 *J. Appl. Cryst.* **50** 959–66
- [34] Coelho A 2018 TOPAS and TOPAS-Academic: an optimization program integrating computer algebra and crystallographic objects written in C++ *J. Appl. Crystallogr.* **51** 210–8
- [35] Bonaccorso A D, Papargyriou D, Cuesta A F, Magdysyuk O V, Michalik S, Connolley T, Payne J L and Irvine J T S 2021 Time-Resolved In-situ X-ray Diffraction Study of CaO and CaO:Ca₃Al₂O₆ composite catalysts for biodiesel production (dataset) (available at: <https://doi.org/10.17630/313c6d61-f04d-4deb-9974-1d2dda459c12>)
- [36] Ramachandran V S, Sereda P J and Feldman R F 1964 Mechanism of hydration of calcium oxide *Nature* **201** 288–9
- [37] Arzamendi G, Arguinarena E, Campo I, Zabala S and Gandia L M 2008 Alkaline and alkaline-earth metals compounds as catalysts for the methanolysis of sunflower oil *Catal. Today* **133–135** 305–13
- [38] León-Reina L, Cabeza A, Rius J, Maireles-Torres P, Alba-Rubio A C and Granados M L 2013 Structural and surface study of calcium glyceroxide, an active phase for biodiesel production under heterogeneous catalysis *J. Catal.* **300** 30–6
- [39] Reyero I, Arzamendi G and Gandia L M 2014 Heterogenization of the biodiesel synthesis catalysis: CaO and novel calcium compounds as transesterification catalysts *Chem. Eng. Res. Des.* **92** 1519–30
- [40] Furusawa T, Kurayama F, Handa H, Kadota R, Sato M and Suzuki N 2014 Transesterification of rapeseed oil with methanol using CaO and active carbon powders encapsulated microcapsule under the light irradiation *Appl. Catal. A* **475** 69–75
- [41] Endale A K, Kiros Y and Zanzi R 2011 Heterogeneous catalysis for biodiesel production from *Jatropha curcas* oil (JCO) *Energy* **36** 2693–700
- [42] Umdu E S and Seker E 2012 Transesterification of sunflower oil on single step sol–gel made supported CaO catalysts: effect of basic strength and basicity on turnover frequency *Bioresour. Technol.* **106** 178–81